TECHNICAL NOTE

Magnetic Resonance in Medicine

Improved abdominal T1 weighted imaging at 0.55T

Bilal Tasdelen¹ | Nam G. Lee¹ | Sophia X. Cui² | Krishna S. Nayak¹

¹Ming Hsieh Department of Electrical and Computer Engineering, University of Southern California, Los Angeles, California, USA

²Siemens Medical Solutions USA, Los Angeles, California, USA

Correspondence

Bilal Tasdelen, Ming Hsieh Department of Electrical and Computer Engineering, University of Southern California, Los Angeles, CA 90089-2564, USA. Email: tasdelen@usc.edu

Funding information

National Science Foundation, Grant/Award Number: 1828736

Abstract

Purpose: Breath-held fat-suppressed volumetric T1-weighted MRI is an important and widely-used technique for evaluating the abdomen. Both fat-saturation and Dixon-based fat-suppression methods are used at conventional field strengths; however, both have challenges at lower field strengths (<1.5T) due to insufficient fat suppression and/or inadequate resolution. Specifically, at lower field strengths, fat saturation often fails due to the short T1 of lipid; and Cartesian Dixon imaging provides poor spatial resolution due to the need for a long Δ TE, due to the smaller Δ f between water and lipid. The purpose of this work is to demonstrate a new approach capable of simultaneously achieving excellent fat suppression and high spatial resolution on a 0.55T whole-body system.

Methods: We applied 3D stack-of-spirals Dixon imaging at 0.55T, with compensation of concomitant field phase during reconstruction. The spiral readouts make efficient use of the requisite ΔTE . We compared this with 3D Cartesian Dixon imaging. Experiments were performed in 2 healthy and 10 elevated liver fat volunteers.

Results: Stack-of-spirals Dixon imaging at 0.55T makes excellent use of the required Δ TE, provided high SNR efficiency and finer spatial resolution $(1.7 \times 1.7 \times 5 \, \text{mm}^3)$ compared Cartesian Dixon $(3.5 \times 3.5 \times 5 \, \text{mm}^3)$, within a 17-s breath-hold. We observed successful fat suppression, and improved definition of structures such as the liver, kidneys, and bowel.

Conclusion: We demonstrate that high-resolution single breath-hold volumetric abdominal T1-weighted imaging is feasible at 0.55T using spiral sampling and concomitant field correction. This is an attractive alternative to existing Cartesian-based methods, as it simultaneously provides high-resolution and excellent fat-suppression.

KEYWORDS

0.55 tesla, abdominal MRI, fat suppression, fat-water separation, mid-field MRI

A preliminary version of this work was presented at ISMRM 2024 #425 (oral presentation).

This is an open access article under the terms of the Creative Commons Attribution License, which permits use, distribution and reproduction in any medium, provided the original work is properly cited.

© 2024 The Author(s). Magnetic Resonance in Medicine published by Wiley Periodicals LLC on behalf of International Society for Magnetic Resonance in Medicine.

Magn Reson Med. 2024;1–8. wileyonlinelibrary.com/journal/mrm

1 | INTRODUCTION

The role of fat-suppressed T1-weighted 3D-GRE abdominal imaging is well established, ^{1–3} with applications from liver tumor detection, surgical planning, to evaluation of pancreatic disease. Imaging is often performed pre- and/or post-contrast. Fat suppression is critical because adipose tissue signals (bright due to their short T1) can obscure normal and abnormal anatomy of interest. Spectrally selective fat-suppression techniques (e.g., Fat-Sat) provide adequate fat suppression at conventional field-strengths (1.5T, 3T) for most applications. For cases where excellent fat-suppression is required, multi-echo Dixon-based techniques (e.g., T1w-Dixon volume interpolated breath-hold examination [VIBE]) are used⁴ at the cost of increased scan time.

At lower field strengths (<1.5T), both of these fat-suppression techniques fail due to the shorter fat T1 (\sim 150 ms)⁵ and smaller chemical-shift between fat and water (-80 Hz).⁶⁻⁸ Spectrally selective saturation fails because the short T1 requires repetition of this preparation more frequently, reducing scan efficiency. Cartesian Dixon imaging provides excellent fat-suppression, but the increased optimal echo separation Δ TE (due to the shorter chemical shift Δ f between water and lipid) requires compromising the spatial resolution to fit the acquisition within a single breath-hold.⁷ A recent study by Ramachandran et al.⁹ evaluated the diagnostic quality of abdominal imaging at 0.55T, and specifically identified fat-suppressed T1-weighted imaging as an area requiring improvement in order to be clinically comparable to higher fields.

In this work, we investigate the use of 3D stack-of-spirals Dixon imaging to simultaneously provide high spatial resolution and excellent fat suppression. The use of spiral sampling¹⁰ is appropriate for its efficiency and because it makes full use of the increased inter-echo spacing. We demonstrate four-fold finer in-plane resolution compared to Cartesian Dixon imaging, while keeping the same breath-hold duration and fat suppression.

2 | METHODS

Experiments were performed using a whole-body 0.55T system (prototype ramped-down MAGNETOM Aera, Siemens Healthineers, Erlangen, Germany) equipped with high-performance shielded gradients (45 mT/m amplitude, 200 T/m/s slew rate). Data collection used a six-channel body array (anterior) and 6 or 12 elements from a table-integrated 18-channel spine array (posterior), depending on the subject's size and position on the table. All imaging was performed without contrast, and in the supine arms-down position. Two healthy volunteers (one

male/one female, male age = 51 y, female age = 21 y, male body mass index [BMI] = 22.3, female BMI = 22) and 10 volunteers with elevated liver fat (4 males/6 females, age range 37-71 y, BMI range 24.7-49.1), were scanned under a protocol approved by our Institutional Review Board, after providing written informed consent.

All scans were RF-spoiled multi-echo gradient-recalled echo and covered a single 26-28 cm axial slab of the abdomen from the top of the liver to the iliac crest. Cartesian-VIBE and Siemens work-in-progress stack-of-spirals-VIBE protocols were designed to utilize the same 16- to 18-s breath-hold duration. We investigate the use of spiral sampling¹⁰ because it makes efficient use of the increased inter-echo spacing at 0.55T, as illustrated in Figure S1. To achieve a multi-echo acquisition, each stack-of-spirals arm was rewound, and the same stack-of-spirals arm was acquired at three echo-times. We acquired each k_z partition with linear order. Within each k_z partition, we acquired spiral interleaves with a linear angle order. The stack-of-spirals acquisition is two-fold undersampled in-plane (k_x, k_y) , and fully sampled through-plane (k_z) . Cartesian Fat-Sat-VIBE (FS-VIBE) was collected on one healthy volunteer. The fat saturation pulse had the same envelope as typically used at 1.5T, 11 and was repeated every 126 ms (10 TRs), to compensate for the shorter T1 of lipid at 0.55T. Both FS-VIBE and Cartesian-Dixon-VIBE used controlled aliasing in parallel imaging results in higher acceleration (CAIPIR-INHA) sampling¹² with an acceleration factor of 3 along the partition encoding direction and 6/8 partial phase Fourier sampling along phase encode direction. Table 1 summarizes the scan parameters.

For spiral acquisitions, the individual echo images are reconstructed using iterative SENSE with L2-norm regularization in BART.¹³ The reconstruction was performed slice-by-slice by taking the Fourier transform along the partition direction (to avoid costly 3D NUFFT's), before the iterative reconstruction. Coil sensitivities are estimated from low-resolution non-linear inversion (NLINV)¹⁴ reconstruction. Surface coil intensity correction is applied using the calibration scans.¹⁵ Exploiting the fact that all scans are prescribed axial, through-plane concomitant fields are corrected by removing the time-dependent phase terms along the readout, as discussed in King et al. 16 2D Gradient non-linearity is corrected by image-based interpolation using the calculated displacement maps, using cubic interpolation. Water/Fat separation is performed using region-growing IDEAL¹⁷ as implemented in the open-source 2012 ISMRM Water/Fat Reconstruction Toolbox.¹⁸ Aliasing from arms is reduced using region-optimized virtual (ROVir) coils.¹⁹ Both arms are manually selected as the interference region, and the body is selected as signal region. We define rectangular

TABLE 1 Sequence parameters for Cartesian Dixon-VIBE, Spiral Dixon-VIBE, and Cartesian FS-VIBE.

Parameter	Cartesian FS-VIBE	Cartesian Dixon-VIBE	Spiral Dixon-VIBE
TEs	1.95 ms	2.1/6.0/9.9 ms	2.1/6.0/9.9 ms
TR	4.32 ms	12.6 ms	14.8 ms
Base resolution	160	128	256
FOV phase	68%	68%	100%
Slice resolution	5 mm	5 mm	5 mm
Parallel imaging	CAIPIRINHA-3	CAIPIRINHA-3	itSENSE-2
Bandwidth	300 Hz/Px	300 Hz/Px	-
Spiral interleaves	-	-	42
Spiral-out duration	-	-	3000 μs
Fat saturation	Yes	-	-
Lines per shot	10	-	-
Flip angle	12°	16-22°	16-22°

Abbreviations: CAIPIRINHA-3, controlled aliasing in parallel imaging results in higher acceleration reconstruction with three-fold acceleration; itSENSE-2, iterative SENSE reconstruction with two-fold acceleration; VIBE, volume interpolated breath-hold examination.

regions of interest on a mid-axial slice that are then replicated along slice dimension to cover the whole volume. ROVir virtual coils are automatically sorted to maximize the signal-to-interference ratio (SIR). We chose the smallest number of coils such that the SNR reduction was less than 10%. The number of coils selected according to this criterion varied between 8 and 13 across our subjects. Both Cartesian and Spiral images are interpolated to $0.88 \times 0.88 \times 1.25 \text{mm}^3$ grid to reduce pixelation artifact using zero-filling in Cartesian (gridded) k-space, after the reconstruction. Cartesian acquisitions were reconstructed using the online GRAPPA reconstruction and fat/water separation provided by the vendor.

To optimize contrast-to-noise ratio (CNR) and SNR, 11 flip-angles from 4° to 90° were tested in one volunteer using the spiral sequence. Muscle, kidney and liver regions were manually segmented, and mean-signal and contrast were plotted. Experimental results were compared against a spoiled GRE (SPGR) simulation,²¹ and literature reported T1 values for muscle, liver and kidney at 0.55T⁵. The flip angle (FA) for subsequent imaging was picked to maximize liver and muscle SNR.

Image quality between Spiral and Cartesian scans are compared qualitatively in terms of the ability to resolve fine structures and organ boundaries within the abdomen, such as liver, kidneys, pancreas, skeletal muscle, and gastrointestinal tract.

3 | RESULTS

Figure 1 shows the mean-signal and contrast curves for each segmented tissue (solid lines). The measured curves

are validated against SPGR simulation with previously reported T1 and T2 values⁵ (dashed lines). According to these, FA of 16–18° provides the best SNR efficiency in terms of liver and muscle signal, and 22–24° provides the best CNR efficiency, in terms of liver-muscle contrast. A FA of 16° was chosen for subsequent experiments.

Figure 2 shows a comparison between Cartesian FS-VIBE, Cartesian Dixon-VIBE, and spiral-Dixon-VIBE water-only images, using three-axis reformat. FS-VIBE imaging provides adequate spatial resolution with incomplete fat suppression. Cartesian Dixon-VIBE provides excellent fat suppression and comparable contrast but has poor spatial resolution. Severe Gibbs ringing artifacts are observed in Cartesian Dixon-VIBE due to the low spatial resolution. Spiral-Dixon-VIBE imaging simultaneously provides appropriate contrast, excellent fat-suppression, and superb spatial resolution.

Figures 3 and 4 compare representative water-only images of Cartesian-Dixon-VIBE and spiral-Dixon-VIBE imaging for volunteers with elevated liver fat with $21.8\% \pm 2.8\%$ and $11.6\% \pm 2.7\%$ proton density fat fraction (PDFF), respectively. Figure S2 shows images passing through kidneys and the liver for all 10 volunteers with elevated liver fat fraction. These figures demonstrate the proposed techniques' ability to image different body habitus.

4 | DISCUSSION

Fat saturation pre-pulses are impractical at 0.55T, due to the shorter T1 (\sim 150 ms) and smaller fat/water chemical-shift (\sim 80 Hz), as shown in Figure 2.

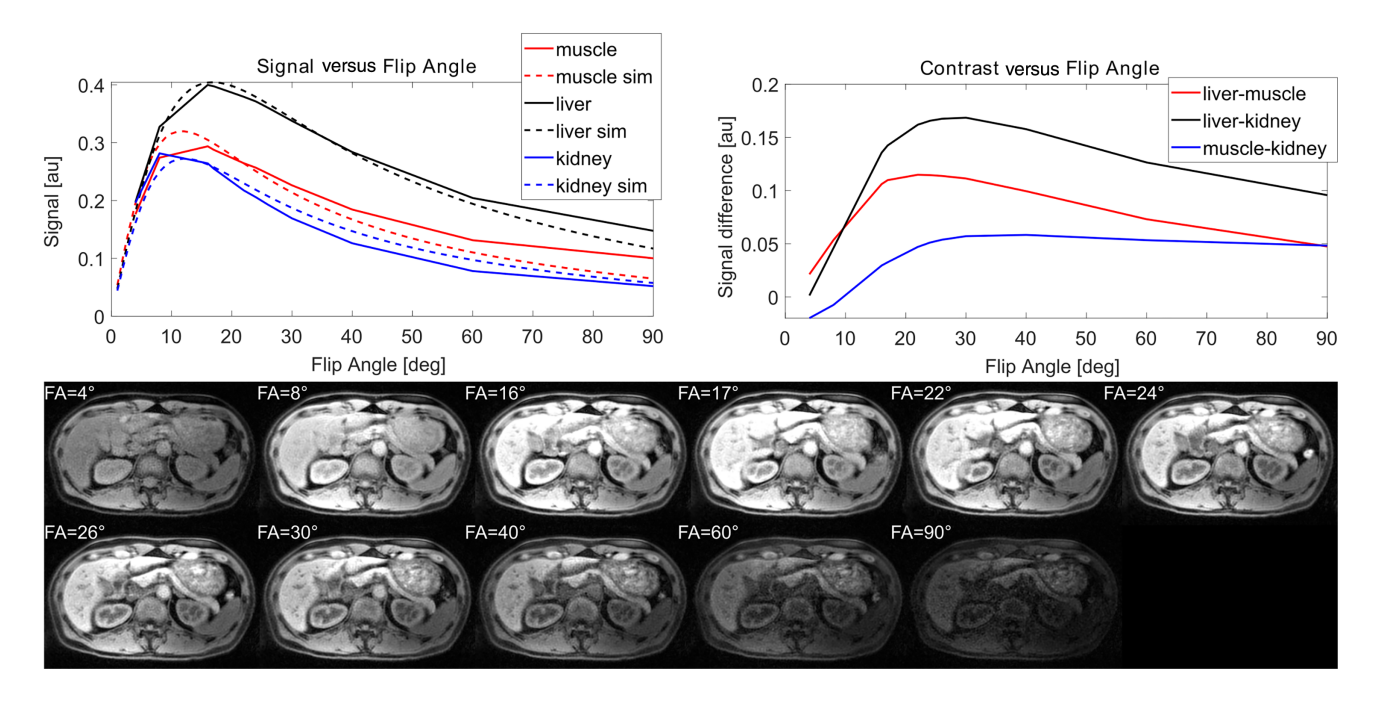


FIGURE 1 Flip angle optimization. Eleven flip angles are tested, spanning the range from 4° to 90°. Liver, skeletal muscle, and kidney are segmented, and average signal from these tissues are plotted as a function of flip angle. Simulated curves (denoted as "sim") are shown with dashed lines. A flip angle of approximately 16° provides the strongest overall signal, and approximately 24° provides the strongest contrast between tissues of interest.

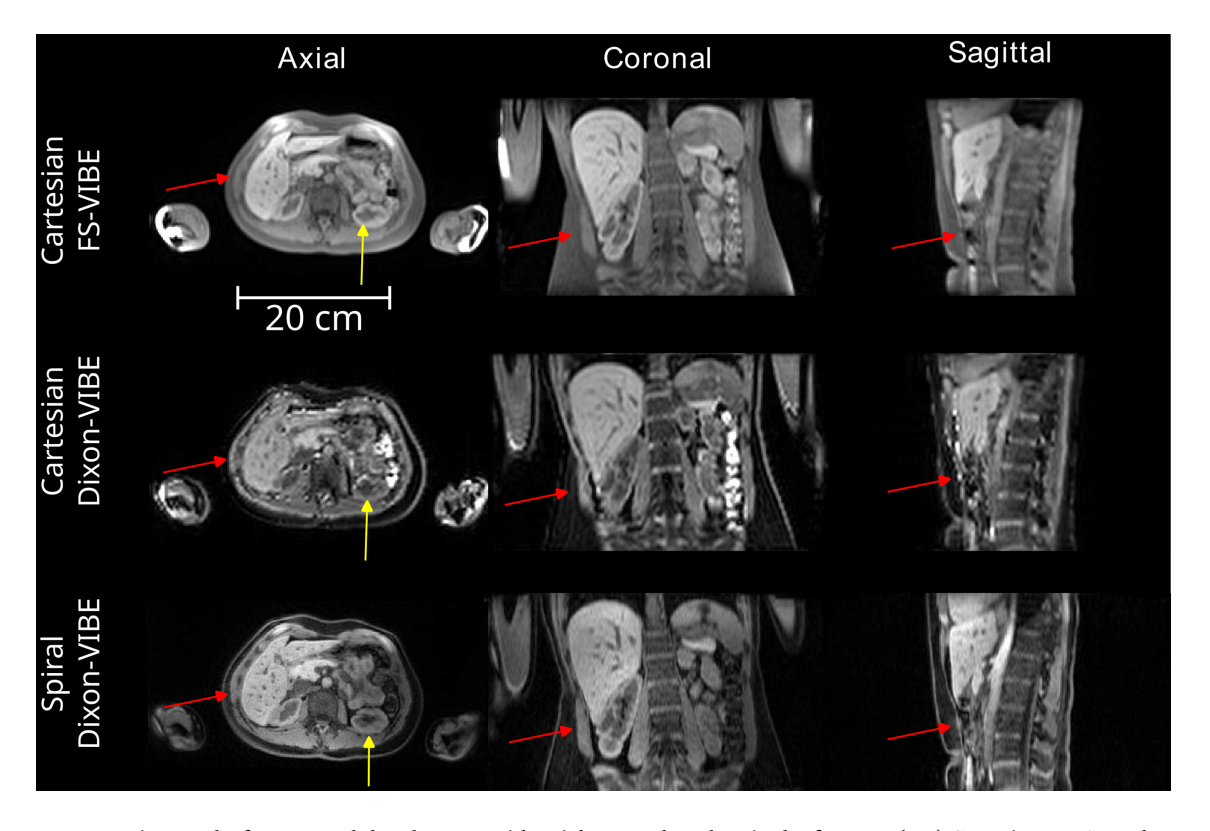


FIGURE 2 In-vivo results from one adult volunteer, with axial, coronal, and sagittal reformats. (top) Cartesian Fat-Sat volume interpolated breath-hold examination (FS-VIBE), (middle) Cartesian Dixon-volume interpolated breath-hold examination (VIBE) water-only, (bottom) spiral-Dixon-VIBE, each acquired in a single 17 s breath-hold. Fat-Sat provides insufficient fat suppression, and poor contrast between subcutaneous fat and muscle (red arrows) due to short T1 and the reduced chemical shift between water and lipid (80 Hz) at 0.55T. Cartesian and spiral Dixon-VIBE provide excellent fat suppression. Only spiral imaging provides the spatial resolution necessary to resolve fine structures and sharp boundaries (yellow arrows) within a clinically practical breath-hold.

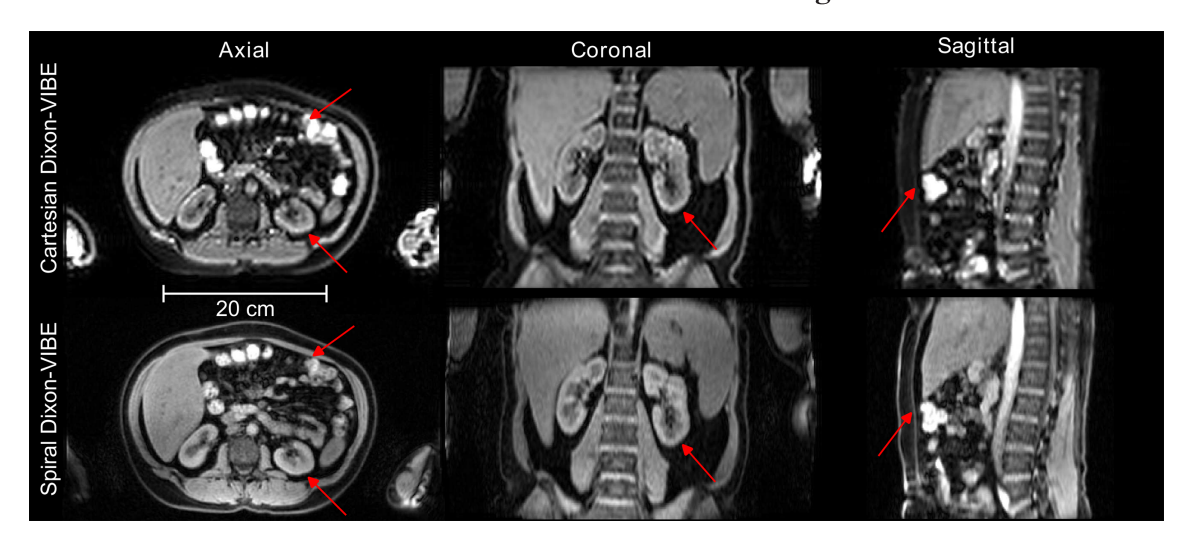


FIGURE 3 In-vivo comparison of Cartesian and Spiral Dixon-volume interpolated breath-hold examination (VIBE) water-only images from a female subject with significant visceral fat and 22% liver proton density fat fraction (PDFF), with axial, coronal, and sagittal reformats. Red arrows point to fine structures where the improvement in spatial resolution can be appreciated. Movies that pan through the volume are included in Video S1 (axial), Video S2 (coronal), and Video S3 (sagittal).

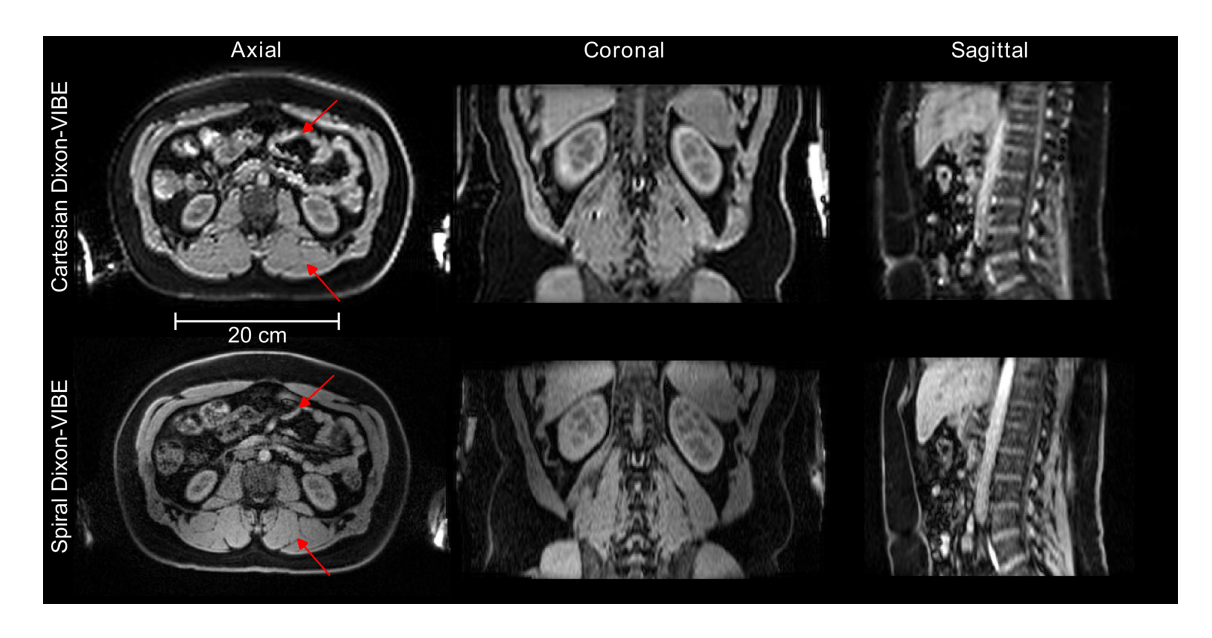


FIGURE 4 In-vivo comparison of Cartesian and Spiral Dixon-volume interpolated breath-hold examination (VIBE) water-only images from a male subject with significant visceral and subcutaneous fat and 12% liver proton density fat fraction (PDFF), with axial, coronal, and sagittal reformats. Red arrows point to fine structures where the improvement in spatial resolution can be appreciated. Movies that pan through the volume are included in Video S4 (axial), Video S5 (coronal), and Video S6 (sagittal).

As an alternative, we demonstrate high resolution, single breath-hold water-only abdominal imaging at 0.55T utilizing spiral-Dixon-VIBE with concomitant field compensation.

There are Fat-Sat pulses tailored for lower fields, however, fundamental limitations mentioned above are still challenging. One issue is the available imaging window being extremely short after each Fat-Sat pulse due to rapid T1-recovery. This causes reduction in scan efficiency, limiting the resolution that can be achieved.

Dixon imaging also provides fat-only images, which may have added value for quantifying visceral fat and other adipose tissue. This could be valuable for risk assessment in some patient groups, such as those with fatty liver disease (Figures 3, 4, Figure S2).

This study shows that it is possible to achieve high-quality abdominal spiral imaging at 0.55T with a combination of concomitant field correction, aliasing reduction (e.g., ROVir), surface coil intensity correction and gradient non-linearity correction. The concomitant

signal loss.

field correction is critical if the echo images are to be used for fat-water separation. Without it, we observed severe fat-water swaps at extreme slices due to the accrued phase between echoes (not shown). ROVir was especially valuable to reduce the aliasing from arms. Without ROVir, it would be necessary to increase the FOV (sacrificing resolution), or image in the arms-up position (sacrificing patient comfort). Note that some intensity shading next to arms is an inevitable side effect of ROVir. A transition region around the interference region always incurs some

For this study, we did not employ additional spiral deblurring methods as we did not observe substantial blurring around gas bubbles in the gastrointestinal tract. The estimated field map from fat-water separation was within $\pm 20\,\mathrm{Hz}$ in the bowel region which will not cause substantial blurring with a relatively short spiral readout of 3 ms. However, the maximum conceivable off-resonance due to air can be around 220 Hz at 0.55T, which results in a 50% wider point spread function than desired. For future studies, this can be mitigated by using more sophisticated reconstruction methods that simultaneously estimate water, fat and field map directly from multi-coil, multi-echo k-space data. ²²⁻²⁴

At lower field strengths, receiver coil arrays tend to have larger elements, and therefore less dense arrays. This is due to the lower center frequency, and to maintain sample noise dominance. This limits opportunities for parallel imaging acceleration.

This study emphasized the demonstration of adequate contrast, fat suppression, and ability to achieve four-fold finer spatial resolution. We applied this to a "catch-all" abdominal protocol in terms of the coverage and resolution. This can be easily adapted to "focused" protocols that cover only liver/pancreas or kidneys/adrenals, and we would expect a similar four-fold increase in spatial resolution over Cartesian-Dixon-VIBE. The proposed method requires broader testing and validation in a larger cohort including diverse clinical cases.

5 | CONCLUSIONS

High resolution single breath-hold volumetric fat suppressed T1 weighted abdominal imaging is feasible at 0.55T using spiral trajectories and concomitant field correction. This approach provides superior spatial resolution compared to Cartesian Dixon-VIBE and superior fat suppression compared to Cartesian fat-suppressed VIBE.

ACKNOWLEDGMENTS

We acknowledge grant support from the National Science Foundation (#1828736) and research support from

Siemens Healthineers. We thank Thomas Benkert and Pan Su for sharing the research stack-of-spirals-VIBE sequence, Liyun Yuan, Darryl Hwang and Vikas Gulani for helpful discussions, and Mary Yung for research coordination.

CONFLICT OF INTEREST STATEMENT

Sophia Cui is an employee of Siemens Healthineers.

DATA AVAILABILITY STATEMENT

Source code and sample raw data are available from the corresponding author, B.T., upon reasonable request. The data that support the findings of this study are openly available in Figshare at http://doi.org/10.6084/m9.figshare.25270669.

ORCID

Bilal Tasdelen https://orcid.org/0000-0001-6462-3651

Nam G. Lee https://orcid.org/0000-0001-5462-1492

Sophia X. Cui https://orcid.org/0000-0002-5133-4903

Krishna S. Nayak https://orcid.org/0000-0001-5735

-3550

REFERENCES

- 1. Rofsky NM, Lee VS, Laub G, et al. Abdominal MR imaging with a volumetric interpolated breath-hold examination. *Radiology*. 1999;212:876-884. doi:10.1148/radiology.212.3.r99se34876
- Conversano F, Franchini R, Demitri C, et al. Hepatic vessel segmentation for 3D planning of liver surgery: experimental evaluation of a new fully automatic algorithm. *Acad Radiol*. 2011;18:461-470. doi:10.1016/j.acra.2010.11.015
- Koç U, Ocakoğlu G, Algın O. The efficacy of the 3-dimensional VIBE-CAIPIRINHA-Dixon technique in the evaluation of pancreatic steatosis. *Turk J Med Sci.* 2020;50:184-194. doi:10.3906/sag-1909-83
- Ding Y, Rao SX, Chen CZ, Li RC, Zeng MS. Usefulness of two-point Dixon fat-water separation technique in gadoxetic acid-enhanced liver magnetic resonance imaging. World J Gastroenterol. 2015;21:5017-5022. doi:10.3748/wjg.v21.i16.5017
- Campbell-Washburn AE, Ramasawmy R, Restivo MC, et al. Opportunities in interventional and diagnostic imaging by using high-performance low-field-strength MRI. *Radiology*. 2019;293:384-393. doi:10.1148/radiol.2019190452
- Baudouin CJ, Bryant DJ, Young IR. Fat suppression in magnetic resonance imaging at low field strength using binomial pulse sequences. *Br J Radiol*. 1992;65:132-136. doi:10.1259/0007-1285-65-770-132
- Hori M, Hagiwara A, Goto M, Wada A, Aoki S. Low-field magnetic resonance imaging. *Invest Radiol*. 2021;56:669-679. doi:10.1097/RLI.000000000000010
- 8. Arnold TC, Freeman CW, Litt B, Stein JM. Low-field MRI: clinical promise and challenges. *J Magn Reson Imaging*. 2023;57:25-44. doi:10.1002/jmri.28408
- Ramachandran A, Hussain HK, Gulani V, et al. Abdominal MRI on a commercial 0.55T system: initial evaluation and comparison to higher field strengths. *Acad Radiol.* 2024. doi:10.1016/j.acra.2024.01.018

- 10. Mugler JP, Fielden S, Meyer CH, et al. Breath-hold UTE lung imaging using a stack-of-spirals acquisition. Proceedings of the International Society for Magnetic Resonance in Medicine. Vol 23; 2015, Toronto, Ontario, Canada. Abstract available at: https://cds.ismrm.org/protected/15MProceedings /PDFfiles/1476.pdf
- 11. Haase A, Frahm J, Hanicke W, Matthaei D. 1H NMR chemical shift selective (CHESS) imaging. Phys Med Biol. 1985;30:341-344. doi:10.1088/0031-9155/30/4/008
- 12. Breuer FA, Blaimer M, Heidemann RM, Mueller MF, Griswold MA, Jakob PM. Controlled aliasing in parallel imaging results in higher acceleration (CAIPIRINHA) for multi-slice imaging. Magn Reson Med. 2005;53:684-691. doi:10.1002/mrm.20401
- 13. Blumenthal M, Holme C, Roeloffs V, et al. BART Toolbox for Computational Magnetic Resonance Imaging. Published online September 24, 2022. doi:10.5281/ZENODO.592960
- 14. Uecker M, Hohage T, Block KT, Frahm J. Image reconstruction by regularized nonlinear inversion—joint estimation of coil sensitivities and image content. Magn Reson Med. 2008;60:674-682. doi:10.1002/mrm.21691
- 15. Pruessmann KP, Weiger M, Scheidegger MB, Boesiger P. SENSE: sensitivity encoding for fast MRI. Magn Reson Med. 1999;42:952-962.
- 16. King KF, Ganin A, Zhou XJ, Bernstein MA. Concomitant gradient field effects in spiral scans. Magn Reson Med. 1999;41:103-112.
- 17. Yu H, McKenzie CA, Shimakawa A, et al. Multiecho reconstruction for simultaneous water-fat decomposition and T2* estimation. J Magn Reson Imaging. 2007;26:1153-1161. doi:10.1002/jmri.21090
- 18. Hu HH, Börnert P, Hernando D, et al. ISMRM workshop on fat-water separation: insights, applications and progress in MRI. Magn Reson Med. 2012;68:378-388. doi:10.1002/mrm.24369
- 19. Kim D, Cauley SF, Nayak KS, Leahy RM, Haldar JP. Region-optimized virtual (ROVir) coils: localization and/or suppression of spatial regions using sensor-domain beamforming. Magn Reson Med. 2021;86:197-212. doi:10.1002/mrm.28706
- 20. Zhu X, Tomanek B, Sharp J. A pixel is an artifact: on the necessity of zero-filling in fourier imaging. Concepts Magn Reson Part A. 2013;42A:32-44. doi:10.1002/cmr.a.21256
- 21. Winkler ML, Ortendahl DA, Mills TC, et al. Characteristics of partial flip angle and gradient reversal MR imaging. Radiology. 1988;166:17-26. doi:10.1148/radiology.166.1.3275967
- 22. Chao TC, Peng X, Wang D, Pipe JG. Evaluating efficient SENSE algorithms to deblur spiral MRI with fat/water separation. Magn Reson Med. 2023;90:2190-2197. doi:10.1002/mrm.29773
- 23. Brodsky EK, Holmes JH, Yu H, Reeder SB. Generalized k-space decomposition with chemical shift correction for non-cartesian water-fat imaging. Magn Reson Med. 2008;59:1151-1164. doi:10.1002/mrm.21580
- 24. Sutton BP, Noll DC, Fessler JA. Fast, iterative image reconstruction for MRI in the presence of field inhomogeneities. IEEE Trans Med Imaging. 2003;22:178-188. doi:10.1109/TMI.2002.808360

SUPPORTING INFORMATION

Additional supporting information may be found in the online version of the article at the publisher's website.

Figure S1. Pulse sequence diagram for x-gradient axis of (A) Spiral and (B) Cartesian acquisition for a single TR. Notice that Spiral acquisition can efficiently use available gradient strength and inter-echo time to either improve resolution or decrease the total acquisition time by decreasing total number of interleaves to fully sample the k-space. In Cartesian case, as the number of k-space lines does not change, this time can only be used for increasing the SNR by decreasing the imaging bandwidth.

Figure S2. A montage of one representative slice for all 10 volunteers with fatty liver disease, showing water-only and fat-only images. The axial slice was chosen to show kidneys and the liver simultaneously. Notice that the spiral acquisition provides good image quality across a broad range of body habitus. The level of fat suppression is excellent, and sharp features can be resolved due to the fine in-plane resolution. Since the proposed approach employs Dixon-based fat-water separation, fat only images are also available, which may be valuable for studying visceral fat and/or ectopic fat.

Figure S3. Estimated coil maps for the central axial slice in one healthy volunteer. (A) magnitude and (B) phase as estimated by non-linear inversion (NLINV). (C) magnitude and (D) phase after region-optimized virtual (ROVir) transformation. Note that, B and S represents body and spine coils for the actual coils, respectively. C and I represents the channels that are used and the channels that are discarded for the ROVir coils, respectively.

Video S1. Axial comparison of Cartesian and Spiral Dixon-volume interpolated breath-hold examination (VIBE) water-only images from a female subject with significant visceral fat and 22% liver proton density fat fraction (PDFF), also shown in Figure 3.

Video S2. Coronal comparison of Cartesian and Spiral Dixon-volume interpolated breath-hold examination (VIBE) water-only images from a female subject with significant visceral fat and 22% liver proton density fat fraction (PDFF), also shown in Figure 3.

Video S3. Sagittal comparison of Cartesian and Spiral Dixon-volume interpolated breath-hold examination (VIBE) water-only images from a female subject with significant visceral fat and 22% liver proton density fat fraction (PDFF), also shown in Figure 3.

Video S4. Axial comparison of Cartesian and Spiral Dixon-volume interpolated breath-hold examination (VIBE) water-only images from a male subject with significant visceral and subcutaneous fat and 12% liver proton density fat fraction (PDFF), also shown in Figure 4.

Video S5. Coronal comparison of Cartesian and Spiral Dixon-VIBE water-only images from a male subject with significant visceral and subcutaneous fat and 12% liver proton density fat fraction (PDFF), also shown in Figure 4.

Video S6. Sagittal comparison of Cartesian and Spiral Dixon-volume interpolated breath-hold examination (VIBE) water-only images from a male subject with significant visceral and subcutaneous fat and 12% liver proton density fat fraction (PDFF), also shown in Figure 4.

How to cite this article: Tasdelen B, Lee NG, Cui SX, Nayak KS. Improved abdominal T1 weighted imaging at 0.55T. *Magn Reson Med*. 2024;1-8. doi: 10.1002/mrm.30224